

1 **The impact of Spike mutations on SARS-CoV-2 neutralization**

2 *Rees-Spear C¹, Muir L¹, Griffith SA¹, Heaney J², Aldon Y³, Snitselaar JL³, Thomas P¹, Graham C⁴,
3 Seow J⁴, Lee N¹, Rosa A⁵, Roustan C⁵, Houlihan CF^{2,6}, Sanders RW³, Gupta R⁸, Cherepanov P⁵, Stauss
4 H¹, Nastouli E^{2,5,8} on behalf of the SAFER Investigators¹, Doores KJ⁴, van Gils MJ³, McCoy LE^{1*}*

5 *¹Institute of Immunity and Transplantation, Division of Infection and Immunity, University College
6 London, UK*

7 *²Advanced Pathogens Diagnostic Unit, Department of Clinical Virology, University College London
8 Hospitals NHS Foundation Trust, UK*

9 *³Department of Medical Microbiology, Academic Medical Center, University of Amsterdam,
10 Amsterdam Institute for Infection and Immunity, Netherlands*

11 *⁴School of Immunology & Microbial Sciences, King's College London, UK*

12 *⁵The Francis Crick Institute, UK*

13 *⁶Research Department of Infection, Division of Infection and Immunity, University College London*

14 *⁷Department of Medicine, University of Cambridge, UK*

15 *⁸Great Ormond Street Institute for Child Health, Infection, Immunity and Inflammation, University
16 College London*

17 *[†]SAFER Investigators are listed in the supplementary information*

18 **Correspondence: L.mccoy@ucl.ac.uk*

19 **Abstract**

20 Multiple SARS-CoV-2 vaccines have shown protective efficacy, which is most likely mediated by
21 neutralizing antibodies recognizing the viral entry protein, Spike. Antibodies from SARS-CoV-2
22 infection neutralize the virus by focused targeting of Spike and there is limited serum cross-
23 neutralization of the closely-related SARS-CoV. As new SARS-CoV-2 variants are rapidly
24 emerging, exemplified by the B.1.1.7, 501Y.V2 and P.1 lineages, it is critical to understand if
25 antibody responses induced by infection with the original SARS-CoV-2 virus or the current
26 vaccines will remain effective against virus variants. In this study we evaluate neutralization of
27 a series of mutated Spike pseudotypes including a B.1.1.7 Spike pseudotype. The analyses of a
28 panel of Spike-specific monoclonal antibodies revealed that the neutralizing activity of some
29 antibodies was dramatically reduced by Spike mutations. In contrast, polyclonal antibodies in
30 the serum of patients infected in early 2020 remained active against most mutated Spike
31 pseudotypes. The majority of serum samples were equally able to neutralize the B.1.1.7 Spike
32 pseudotype, however potency was reduced in a small number of samples (3 of 36) by 5-10-
33 fold. This work highlights that changes in the SARS-CoV-2 Spike can alter neutralization
34 sensitivity and underlines the need for effective real-time monitoring of emerging mutations
35 and their impact on vaccine efficacy.

36 **Introduction**

37 Serum neutralization activity is a common correlate of protection against viral infection
38 following vaccination or natural infection (Plotkin, 2008). However, effective protection from
39 viral infection can also require sufficient breadth of serum neutralization rather than potency
40 alone. This is because of the high-levels of variation observed in major antigens across some
41 viral populations (Burton, Poignard, Stanfield, & Wilson, 2012). The classic example in which a
42 lack of breadth limits the protective capacity of the antibody response is Influenza. Here, the
43 majority of neutralizing serum antibodies target only a particular set of influenza strains as a
44 result of antigenic drift of the immunodominant hemagglutinin head (Zost, Wu, Hensley, &
45 Wilson, 2019). Due to this, an annual vaccine is required and must be matched to the most
46 probable circulating strain in any given year to ensure protection from infection. Emerging data
47 from human vaccine trials and challenge studies in animal models suggest that neutralizing
48 antibodies can prevent disease caused by infection with SARS-CoV-2, the virus that causes
49 COVID-19 (McMahan et al., 2020; Polack et al., 2020). However, new variants of SARS-CoV-2
50 have begun to emerge in both human and farmed animal populations (S. Kemp et al., 2020;
51 Oude Munnink et al., 2020; Tegally et al., 2020; Welkers, Han, Reusken, & Eggink, 2020). These
52 variants include mutations in the major neutralizing antigen, the Spike glycoprotein, and raises
53 the question of whether neutralizing serum responses induced by early circulating strains or by
54 vaccines based on the Spike sequence of these early strains can neutralize the recently emerged
55 virus variants.

56 Prior to the emergence of multiple mutations in Spike in the human population, we
57 reasoned that a logical way to identify potential escape mutations was to look at sites of amino
58 acid variation relative to the most closely related human betacoronavirus SARS-CoV, which
59 caused the original SARS outbreak in 2003 (CDC, 2003). These two closely related viruses are
60 characterized by a notable difference in transmission dynamics and disease outcomes (Cevik,
61 Kuppalli, Kindrachuk, & Peiris, 2020; Lipsitch et al., 2003; Petersen et al., 2020) but both use
62 the human ACE2 protein as a viral entry receptor (W. Li et al., 2003) and share approximately
63 75% similarity overall in Spike at an amino acid level (Gralinski & Menachery, 2020). Both
64 viruses use the same region of their respective Spikes to bind ACE2; the receptor binding
65 domain (RBD - found within the S1 subunit of Spike). There is considerable amino acid
66 variation between the two RBDs, despite their conserved binding to ACE2, which explains why
67 the majority of SARS-CoV-induced neutralizing monoclonal antibodies (mAbs) were found not
68 to neutralize SARS-CoV-2, although some cross-binding activity has been observed (Wu et al.,
69 2020) and targeted mutations can enable neutralization (Liu et al., 2020). Similarly, the

70 majority of COVID-19 sera have either weaker or no neutralizing activity against SARS-CoV, but
71 cross-neutralizing mAbs have been isolated (Brouwer et al., 2020).

72 Since the start of the pandemic, sequencing of viral populations has been deployed to
73 enable detection of individual mutations within SARS-CoV-2 and identify new variants or
74 strains that become dominant. Most recently, a new variant, B.1.1.7, has emerged in the UK (S.
75 Kemp et al., 2020; Rambaut et al., 2020) that includes multiple mutations in both the RBD and
76 the N-terminal domain (NTD) of Spike, both targets for neutralizing antibodies. Similarly, two
77 further variants have been identified in South Africa, 501Y.V2, and Brazil, P.1, which carry
78 additional mutations in both the NTD and RBD (Faria et al., 2021; Tegally et al., 2020). All three
79 variants share a deletion of 3 amino acids in Orf1ab and key mutations in the RBD (E484K and
80 the N501Y); data so far consistent with convergent evolution. Early reports have indicated that
81 while the RBD mutation N501Y in the B.1.1.7 strain does not compromise post vaccine serum
82 neutralization (Xie et al., 2021), one of the individual changes in the 501Y.V2 strain does impair
83 neutralization but does not remove all activity (Greaney et al., 2021). Moreover, *in vitro* escape
84 studies have shown similar mutations occur under selective pressure (Andreano et al., 2020).

85 Therefore, in this study we evaluated the potential role of individual amino acids in
86 facilitating escape from neutralizing antibodies. Firstly, by making a series of point mutations to
87 change the amino acids in SARS-CoV-2 to those found at the analogous position in SARS-CoV.
88 Secondly, by making individual point mutations emerging in real world populations and by
89 generating a pseudotype virus using the B.1.1.7 variant Spike sequence. We identify multiple
90 mutations that can abrogate neutralization by some monoclonal antibodies targeting the RBD
91 of Spike. However, in contrast, we show that serum responses are more resilient to these
92 mutations, especially following severe infection where the antibody response is characterized
93 by increased breadth.

94 **Results**

95 **Generation of potential escape mutants by SARS-CoV amino acids substitution**

96 There are 56 individual amino acid changes between the RBD of SARS-CoV-2 and SARS-CoV
97 (Ortega, Serrano, Pujol, & Rangel, 2020), including sites at which antibody escape has been
98 observed for SARS-CoV (Rockx et al., 2010). We identified 15 sites where single, or sequential,
99 non-conservative amino acid changes were observed compared to SARS-CoV. These sites were
100 mutated in the SARS-CoV-2 Spike to match SARS-CoV (Fig S1). Mutated Spike protein plasmids
101 were then co-transfected with a lentiviral construct encoding luciferase and a packaging
102 plasmid to produce pseudotyped viruses (Seow et al., 2020). Three of the substitutions
103 resulted in virus that did not give sufficient titer to evaluate the impact on neutralization

104 activity. The remaining mutated pseudotypes were then screened for any alteration in
105 neutralization against a panel of human mAbs (Brouwer et al., 2020) isolated post SARS-CoV-2
106 infection. These mAbs have been previously mapped into eleven binding clusters whereby
107 mAbs within a cluster reciprocally compete for binding to Spike. Of these, eight clusters
108 comprise neutralizing mAbs (I, III, IV, VI, VII, IX, X, XI), five of which target the RBD (I, III, VI, VII,
109 IX), and three clusters contain only non-neutralizing mAbs (II, V and VIII). Representatives of
110 each neutralizing cluster were selected for evaluation against the Spike mutant pseudotypes.

111 **Impact of SARS-CoV Spike substitutions on SARS-CoV-2 mAb neutralization**

112 Initial screening assays of the twelve infectious viral pseudotype mutants showed no effect
113 on neutralization by any of the mAbs against three mutants with changes at amino acid
114 positions RFA₃₄₆₋₈KFP, S₄₅₉G, and ST₄₇₇₋₈GK (FigS1). In contrast, the remaining nine viral
115 pseudotype mutants diminished neutralization for at least one mAb (Fig1) as described below:

116 **P₃₈₄A**

117 The P₃₈₄A substitution resulted in complete loss of neutralization by COVA1-16 (Fig1A), a
118 cluster III RBD-specific mAb that allosterically competes with ACE2 rather than directly
119 blocking the binding site (Liu et al., 2020). Of note, this mutation has been described and
120 structurally characterized elsewhere (Wu et al., 2020), revealing that this proline to alanine
121 change results in a relatively small alteration in protein structure that can enable SARS-CoV
122 mAbs to neutralize SARS-CoV-2 P₃₈₄A. However, P₃₈₄A does not weaken neutralization by any
123 other mAbs, including another mAb in the cluster III competition group.

124 **K₄₁₇V**

125 The K₄₁₇V mutation results in a pseudotyped virus that is less susceptible to COVA2-07
126 mediated neutralization, which is the other cluster III RBD-specific mAb screened (Fig1A).
127 COVA2-07 belongs to the same sub-cluster as COVA2-04, the structure of which has been solved
128 and contact residues include numerous bonded and non-bonded contacts within the RBD and
129 ACE2-binding site (Wu et al., 2020). That this mutation should alter mAbs such as COVA2-07,
130 which competes directly with ACE2 for binding, is not unexpected as the lysine at position 417
131 forms a hydrogen bond with ACE2 (Lan et al., 2020) that is likely disrupted by this substitution.
132 We then evaluated an additional mAb, COVA2-04, from the same competitive binding cluster as
133 COVA2-07. This is because COVA2-04 is representative of class of SARS-CoV-2 neutralizing
134 antibodies that all use the VH3-53 gene and have been suggested to be an unusual “public” or
135 stereotyped antibody (Cao et al., 2020; Mor et al., 2020; Robbiani et al., 2020). COVA2-04 was
136 not able to neutralize the K₄₁₇V pseudotype (data not shown). Although, of note, this mutation
137 has no real impact on neutralization by any of the other mAbs tested.

138 **KVG₄₄₄₋₆TST**

139 This multiple substitution, which is a substantial change between SARS-CoV-2 and SARS-
140 CoV, results in a 3.7-fold drop in neutralization potency for COVA2-29, which is a cluster I RBD-
141 specific antibody (Fig1A, B). This is the largest effect of this mutation, as the neutralization
142 activity of the other mAbs is largely unaffected despite the alteration of three sequential amino
143 acids. This may be explained by the relatively minor differences in the amino acid side chains at
144 the mutated residues. Unlike some of the other mutants tested, such as LF₄₅₅YL that introduces
145 a phenol, the substitutions made here may not disrupt protein structure or antibody binding to
146 any great extent. Notably, binding analysis has suggested mutations in this loop can reduce RBD
147 binding by Spike-specific sera (Greaney et al., 2021).

148 **L₄₅₂K**

149 This mutation is situated directly within the receptor binding motif (RBM) of the RBD. It
150 renders pseudotyped virus resistant to neutralization by the cluster I mAb COVA2-29, but does
151 not affect the other cluster I mAb COVA1-18 or any other mAb tested.

152 **LF₄₅₅YL**

153 This double substitution reduces neutralization by RBD-specific mAbs from different clusters,
154 specifically, the cluster I mAb COVA2-29, cluster III mAb COVA2-07 and cluster VI mAb COVA1-
155 12 (Fig1A, B). For COVA1-12 all neutralization activity is abolished, while COVA2-07 activity is
156 just below the level required to calculate an IC₅₀ value.

157 **TEI₄₇₀₋₂NVP**

158 This triple mutation is located in a loop within the RBM where other substitutions have been
159 reported to abolish ACE2 binding (Xu et al., 2021; Yi et al., 2020). This mutation prevents
160 neutralization by COVA2-29 (cluster I), COVA2-07 (cluster III) and COVA2-02 (cluster VII). It
161 also reduces the activity of the most potent mAb COVA1-18 (cluster I) by 3-fold, whereas this
162 mAb is only minimally affected by other mutations. Moreover, TEI₄₇₀₋₂NVP lowers the potency
163 of the structurally unmapped non-RBD cluster XI mAb, COVA1-21, to the limit of detection.
164 Thus, this mutation negatively impacts the most mAbs, including representatives from four
165 separate epitope clusters.

166 **S₄₉₄D**

167 This single substitution towards the end of the RBM destroys neutralization activity by both
168 COVA2-29 (cluster I) and COVA1-12 (cluster VI) but does not have a major impact on the other
169 cluster I mAb tested or those from other epitope clusters.

170 In summary, different mAbs can lose their neutralization activity when confronted with
171 different Spike mutations and the effects are not strictly delineated by binding clusters, such

172 that mAbs within the same competition cluster are frequently differentially affected. The triple
173 substitution TEI₄₇₀₋₂NVP has the most detrimental effects on different antibodies and impacts
174 mAbs from nearly all binding clusters. LF₄₅₅YL also negatively affects mAbs across different
175 binding clusters. Notably, COVA2-29 is the mAb that is most frequently negatively affected by
176 different mutations, with substantial loss of some neutralizing activity against four mutations
177 (L₄₅₂K, LF₄₅₅YL, TEI₄₇₀₋₂NVP, S₄₉₄D), which are all within the RBM of the RBD (Fig1A). COVA2-29
178 is also known to compete directly with ACE2 for binding to Spike, which may explain why it is
179 sensitive to so many different mutations within the RBM.

180 **Impact of Spike mutations on serum neutralization**

181 Following the identification of Spike mutations that can limit or abrogate neutralizing
182 activity of mAbs (Fig2A), the next step was to assess the impact of these mutations on serum
183 neutralization. Samples were tested following two different infection scenarios. Firstly, from a
184 previously characterized cohort of seropositive healthcare workers who experienced mild or
185 asymptomatic SARS-CoV-2 infection (Houlihan et al., 2020). Secondly, sera were obtained from
186 a cohort of hospitalized patients who experienced severe disease. Eighteen samples were
187 chosen from both cohorts for screening purposes to obtain representatives with intermediate
188 (1:50-100), strong (1:100-1000) and potent (>1:1000) neutralizing ID₅₀ values. The median
189 serum ID₅₀ for hospitalized patients selected was 1:1275, and that for selected
190 mild/asymptomatic cases was 1:1045. Strikingly, serum samples from both cohorts are less
191 impacted by Spike mutations than individual mAbs in terms of fold decrease in neutralization
192 potency (Fig2B and C). Only one of thirty-six serum samples lost all neutralizing activity (Fig
193 S2), in contrast to the five mAbs from five different epitope clusters where neutralization was
194 completely abrogated by a single Spike mutation (Fig 1B). Moreover, fold-decrease in
195 neutralization potency was more modest for sera than mAbs, with an average 2-fold decrease
196 across all sera for the most disadvantageous mutation TEI₄₇₀₋₂NVP as compared to a more than
197 100-fold decrease observed for several of the mAbs (Fig2B and C). Interestingly, none of the 36
198 serum samples lost >5-fold potency against the other triple substitution, KVG₄₄₄₋₆TST which
199 contrasts with recent data showing a single mutation at G₄₄₆ caused a major loss of
200 neutralization in one sample (Greaney et al., 2021). Importantly, there was notable difference
201 between the resilience of serum samples from severely ill hospitalised individuals and those
202 who had experienced mild/asymptomatic infection. Only two serum sample from a hospitalised
203 individual lost more than 3-fold potency against any individual mutant (Fig2C, FigS2). Whereas
204 approximately half (10 of 18) the mild/asymptomatic serum samples showed a three-fold drop
205 in potency against at least one Spike mutant (Fig2C, Fig S2).

206 **Greater levels of Spike-reactive antibodies in sera after severe illness**

207 The differences in resilience to Spike mutations seen in the neutralizing sera from these
208 two infection scenarios is plausibly due to greater polyclonality arising from greater antigenic
209 stimulation during severe illness. To assess the serological profiles of these two cohorts, we
210 compared the 50% inhibitory dilution (ID_{50}) values across 192 samples and measured the
211 binding titers by semi-quantitative ELISA for 199 samples as previously described (Ng et al.,
212 2020; O'Nions et al., 2020). There is a significantly higher median IgG binding titer of 46.5
213 $\mu\text{g}/\text{ml}$ following severe illness versus 3.9 $\mu\text{g}/\text{ml}$ following mild/asymptomatic disease (Fig3A,
214 FigS3). Similarly, there is a significantly higher median ID_{50} value in the hospitalized patient
215 cohort as compared to the mild/asymptomatic group (Fig3B). This shows, as has been
216 observed previously (Seow et al., 2020), that severely ill patients have higher binding and
217 neutralization titers than asymptomatic/mild cases and that higher binding titers correlate
218 with greater neutralization. However, when considering how the IgG binding titer from each
219 individual relates to their neutralization titer it became clear that there was a discrepancy
220 (Fig3C and D). Most hospitalized patients required a binding titer of greater than 10 $\mu\text{g}/\text{ml}$ to
221 achieve strong neutralization ($ID_{50} > 100$). Moreover, mild infections could lead to potent
222 neutralization ($ID_{50} > 1000$) at binding titers of less than 10 $\mu\text{g}/\text{ml}$ (Fig3D) whereas this was
223 observed for only two individuals following severe illness (Fig3C). In fact, the amount of
224 specific IgG present at the serum ID_{50} is significantly higher in severe illness compared to mild
225 disease (Fig 3E). This suggests that a higher proportion of antibodies are non-neutralizing
226 following severe illness. However, the total level of specific antibodies is so high that the
227 number of neutralizing antibodies following severe illness may be greater and explain the
228 relative resilience of severe sera to Spike mutations.

229 **Impact of Spike variants on mAb and serum neutralization**

230 Investigating the ability of post-SARS-CoV-2-infection mAbs and serum to cope with
231 mutations in Spike engineered based on differences with SARS-CoV was a rational first
232 approach to study escape, because these mutations were likely to form viable Spike proteins.
233 Indeed, some of the positions at which amino acids were mutated, as described above, have
234 now been observed to be a site of variance in SARS-CoV-2 across the human population (Q. Li et
235 al., 2020; Liu et al., 2020; Starr et al., 2020). However, additional viral variants, not linked to
236 points of variance between these two closely related viruses, have started to emerge on a
237 significant scale (Q. Li et al., 2020; Weisblum et al., 2020). Firstly, the D₆₁₄G mutation, observed
238 in western Europe in February 2020 and now dominant across the globe (Korber et al., 2020).
239 It has already been described that D₆₁₄G has higher infectivity and greater viral replication
240 (Korber et al., 2020; Q. Li et al., 2020; Plante et al., 2020) and somewhat increases the ability of
241 serum and mAbs to neutralize SARS-CoV-2 (Korber et al., 2020; Plante et al., 2020; Weissman et
242 al., 2020). More recently, a new variant of SARS-CoV-2 (B.1.1.7) has emerged in England and

243 been associated with a rapid rise in case numbers (S. Kemp et al., 2020; Rambaut et al., 2020)
244 and high viral loads (Kidd et al., 2020). B.1.1.7 encodes 8 sites of change in Spike relative to the
245 original Wuhan strain. Of these, the most likely candidates to alter neutralization sensitivity are
246 the deletion in the NTD ($\Delta H_{69}/V_{70}$) and the $N_{501}Y$ substitution in the RBM (S. Kemp et al., 2020;
247 Rambaut et al., 2020). Therefore, these changes were introduced in the Wuhan strain Spike in
248 the presence of $D_{614}G$ to produce pseudotyped viruses for neutralization sensitivity analysis.
249 Firstly, $\Delta H_{69}/V_{70}$ did not negatively impact the neutralization potency for most of the mAbs
250 tested, including cluster IX mAb COVA2-17 (Fig4A), which has recently been found to bind the
251 NTD (Rosa et al., 2021). The exception was the structurally unmapped COVA1-21 (cluster XI),
252 which was previously reported to lose partial potency against this deletion in the context of
253 other mutations that arose in an immuno-compromised patient (S. A. Kemp et al., 2020).
254 Similarly, the serum neutralization activity did not decrease by more than 3-fold relative to the
255 $D_{614}G$ Spike for any individual sample (Fig4B). In contrast, the introduction of the $N_{501}Y$
256 substitution (observed in both B.1.1.7, 501Y.V2 and P.1) lowered the neutralization potency of
257 one mAb, COVA1-12, to the limit of the assay, with a fold decrease in IC_{50} of >40 (Fig4A). This
258 cluster VI RBD-specific mAb was also negatively impacted by proximal mutations at $LF_{455}YL$
259 and $S_{494}D$. Moreover, a 5-fold decrease in potency was observed against the $N_{501}Y$ pseudotype
260 for the cluster IX mAb COVA2-17, which also loses efficacy against $TEI_{470-2}NVP$. However, as
261 seen for the other mutations that abrogate mAb function, the $N_{501}Y$ change had less of an effect
262 on the sera obtained after both severe and mild infection, with all individual serum samples
263 remaining within three-fold of their original ID_{50} value (Fig4B, FigS4).

264 **Impact of B.1.1.7 Spike on mAb and serum neutralization.**

265 Finally, a B.1.1.7 Spike pseudotyping plasmid was synthesized to incorporate the mutations
266 observed in this new variant in combination, and then evaluate neutralization sensitivity of
267 mAbs and sera. This showed that, as per individual mutants, B.1.1.7 can lessen the potency of
268 some mAbs, although unlike other mutations described above, it does not remove all activity
269 for any individual mAb and in total three mAbs were affected, COVA2-17, COVA1-12 and
270 COVA1-21 (Fig4A). These mAbs belong to distinct clusters and so do not compete for binding to
271 the same epitope. Firstly, the cluster IX mAb COVA2-17 showed an approximate 5-fold drop in
272 potency against both the $N_{501}Y$ single mutant and the B.1.1.7 pseudotype, implying this loss of
273 potency is primarily $N_{501}Y$ driven. In contrast, the decrease in potency noted with the single
274 $N_{501}Y$ change for the RBD-specific mAb COVA1-12 was lessened in the context of B.1.1.7, with a
275 11-fold rather than a >40 -fold drop in neutralization. Furthermore, one mAb, COVA1-21
276 experienced a substantial drop in potency against B.1.1.7 compared to the single mutants or the
277 $D_{614}G$ spike. This cluster XI mAb, which does not bind to RBD or S1 subunits, showed more than
278 100-fold reduction in potency. This effect is likely in part mediated by the $\Delta H_{69}/V_{70}$ deletion

279 that also reduced the potency of COVA1-21 when evaluated as a single mutant. The B.1.1.7
280 Spike was then tested against the 36 serum samples from the two cohorts (Fig4B). The
281 maximum fold-decrease in potency for the serum samples from mild illness was 8.2 but the
282 majority of samples showed less than a 3-fold change. Similarly, the maximum decrease seen
283 for samples from hospitalized patients was a 9.1-fold change, but most of the samples showed
284 minimal change in the potency of their neutralization. Overall, three samples from each cohort
285 (8%) showed a 5–10-fold reduction, but as they were potently neutralizing sera, the reduced
286 ID₅₀ values were still >1:100. Similarly, another four samples from both cohorts (11%) showed
287 a 3–5-fold reduction in neutralization when tested against the B.1.1.7 Spike pseudotype. Again,
288 the reduced ID₅₀ values were still potent (on average >1:500) with only two samples having an
289 ID₅₀ of <1:200 (Fig S4)

290 **Discussion**

291 This study demonstrates that Spike mutations can diminish or abolish neutralizing activity by
292 individual mAbs but that serum neutralization is less strongly affected. Notably, only one
293 engineered mutation, and none of the observed Spike mutants or the B.1.1.7 variant, resulted in
294 a complete escape from neutralizing activity and this was only seen for one out of thirty-six
295 serum samples. The Spike mutants evaluated comprise seven substitutions designed to mimic
296 possible escape changes based on homology with SARS-CoV, two observed high-frequency
297 mutations and the B.1.1.7 Spike variant. The most likely explanation for the greater effect on
298 mAbs as compared to sera is the inherent polyclonality underlying serum neutralization. This
299 concept is supported by the observation that single Spike mutations can weaken neutralization
300 for a particular mAb but not for other mAbs from within the same binding cluster. This
301 highlights that different antibodies use distinct molecular contacts within shared epitopes, such
302 that a single mutation may not be detrimental to all antibodies within the same binding cluster.
303 Thus, because polyclonal sera contain multiple antibodies that target the major neutralizing
304 sites in subtly different ways, it is less sensitive to Spike mutations.

305 The Spike mutations studied here were designed to identify potential escape variants by
306 mimicking in part the natural variation observed between SARS-CoV and SARS-CoV-2, and are
307 focused mainly on the RBD as the major site of neutralizing antibody activity. Therefore, it was
308 unsurprising that many of the RBD-specific mAbs evaluated here lost neutralization activity
309 against one or more of these mutations. These included substantial multi-residue substitutions
310 not yet seen in the SARS-CoV-2 but also single point mutations at positions that have been
311 observed to mutate in the real world (S. Kemp et al., 2020; Korber et al., 2020; Rambaut et al.,
312 2020; Tegally et al., 2020). These include, K₄₁₇V that had a negative effect on mAb
313 neutralization and another mutation at this position, K₄₁₇N, has been observed in the emerging

314 South African variant (Tegally et al., 2020). Importantly, the mAb (COVA2-07) that loses >40-
315 fold neutralization activity against the K₄₁₇V pseudotyped virus belongs to the same cluster as
316 COVA2-04 that loses all neutralization activity against the K₄₁₇V mutant. COVA2-04 belongs to
317 the VH3-53 “public” BCR against SARS-CoV-2 identified from multiple human infections. Thus,
318 COVA2-04-like antibodies are thought to be widespread among the seropositive population and
319 so the K₄₁₇V would be predicted to have an impact on sera from many individuals. Interestingly,
320 serum samples from mild infection showed very little change in neutralization potency against
321 this mutation. However, the strongest effect on serum samples from mild infection was
322 mediated by the TEI₄₇₀₋₂NVP substitution, which is part of what has been termed the RBD
323 binding ridge, and other mutations in this region can decrease serum neutralization (Greaney
324 et al., 2021). As such, any mutation in this zone should be closely monitored in viral populations
325 due to the potential for escape. However, it is encouraging that the effect of these mutations on
326 sera was much less pronounced and that individual mAbs within the same clusters were not
327 universally inactivated by any given mutation. Notably, the mutations that most substantially
328 decrease serum neutralization are those that negatively impact mAb activity against the widest
329 range of clusters (I, III, XI, IX and VI) suggesting that mAb screening is a useful proxy for
330 potential serum effects if a range of antibody clones are used. However, the capacity to predict
331 the *in vivo* impact of a drop in neutralization potency requires correlation of *in vitro* serum
332 neutralization ID₅₀ values with protection, which thus far has only been achieved in animal
333 models where, encouragingly, an ID₅₀ value of 1:50 was found to be protective (McMahan et al.,
334 2020).

335 A caveat to the first part of this study is that only RBD substitutions were considered.
336 Further studies to assess potential mutations before they arise should include those in NTD
337 given the emerging importance of NTD as a site for neutralizing antibodies (Andreano et al.,
338 2020; Rosa et al., 2021). However, it should be noted that one RBD change, TEI₄₇₀₋₂NVP,
339 resulted in a 24-fold drop in potency for COVA1-21, which does not bind RBD and remains
340 structurally unmapped (Brouwer et al., 2020). Regardless, that sera likely containing a mixture
341 of RBD- and NTD-specificities are more resilient than individual mAbs in the face of Spike
342 mutations within the RBD is not surprising. This further highlights the importance of a broad
343 polyclonal serum response to maintain neutralizing activity in the event of novel Spike
344 mutations emerging, and the need to consider more than RBD binding in serological
345 evaluations.

346 To understand if the conclusions from studying the impact of the SARS-CoV-2/SARS-CoV
347 substitutions on neutralization parallel those of real-world Spike mutations, we examined the
348 responses to the newly emerged B.1.1.7 variant (S. Kemp et al., 2020; Rambaut et al., 2020).

349 This revealed that the first NTD deletion observed, $\Delta H_{69}/V_{70}$, did not alter RBD-specific mAbs or
350 any sera. Although as previously described (S. A. Kemp et al., 2020) it did result in a drop in
351 potency for non-RBD mAb COVA1-21. The RBD mutation $N_{501}Y$, shared between B.1.1.7,
352 501Y.V2 and P.1, did remove almost all neutralizing activity for one mAb but, in a similar
353 pattern to other substitutions, this did not translate to any large effect on serum potency. Of
354 note, we have not studied changes at position 484 that have been observed in 501Y.V2 and P.1
355 and reported to reduce neutralization in serum samples (Greaney et al., 2021) and during *in*
356 *vitro* escape (Andreano et al., 2020). Further studies of mutations at position 484 and new
357 emerging mutations will be needed. This would best be facilitated by large, curated panels of
358 mAbs and pools of sera from individuals with different infection/vaccination trajectories.

359 Theoretically it is likely that combinations of mutations have more potential to lead to loss
360 of serum activity than individual single amino acid changes by destroying multiple parts of key
361 epitopes. This has partially been observed in terms of the new B.1.1.7 Spike pseudotype
362 analyzed here. Only one mAb was more dramatically affected by the full set of B.1.1.7
363 mutations. However, the small number of serum samples with reduced neutralization relative
364 to the $D_{614}G$ virus, were more strongly affected by B.1.1.7 than either the $\Delta H_{69}/V_{70}$ or $N_{501}Y$
365 mutations individually (Fig 4B). This reduced neutralization was seen in 11% (3-5-fold) and
366 8% (5-10-fold) when tested against the B.1.1.7 Spike pseudotype. However, all of the affected
367 samples were still able to neutralize B.1.1.7, and the average reduced serum ID_{50} value was
368 1:522. This is ten-times higher than the reported serum ID_{50} correlate of protection in animal
369 studies and suggests these responses would likely still be effective against infection with
370 B.1.1.7.

371 The differences in the data observed with B.1.1.7 and the two individual mutations
372 $\Delta H_{69}/V_{70}$ or $N_{501}Y$ highlight the importance of testing emerging variants in the full form.
373 Moreover, this approach may be important as combinations of mutations could enable
374 individual antibody escape mutations that are disadvantageous for transmission to be
375 propagated. For example, a residue such as S_{494} is involved both in ACE2 binding (Xu et al.,
376 2021) and mAb neutralization (Fig1). Therefore, a mutation at S_{494} could decrease antibody
377 function but also decrease host receptor recognition and limit infectivity. However, the
378 detrimental effects of the mutation on infectivity could be compensated for if a S_{494} mutation
379 occurred in concert with a mutation that strengthened a different part of the viral entry
380 pathway as has been suggested(S. A. Kemp et al., 2020). This highlights the need for rapid
381 evaluation of variant strains upon emergence, potentially accelerated by computational
382 modeling based on prior knowledge of the effects of individual changes.

383 In conclusion, this study underlines both the potential for escape from neutralizing
384 antibodies due to mutations in Spike and the relative resilience of serum responses compared
385 to individual mAbs. This difference likely derives from the breadth inherent in polyclonal sera
386 as compared to the precision interaction of a given mAb. Our results suggest that the majority
387 of vaccine responses should be effective against the B.1.1.7 variant as the sera evaluated were
388 obtained after infection early in the pandemic when the commonly circulating virus was highly
389 similar in sequence to the vaccines now being deployed. A reduction in potency was observed
390 in a minority of samples tested against B.1.1.7, however, neutralization titers remained above
391 1:200 in almost all cases. Finally, it is probable that as SARS-CoV-2 seropositivity increases
392 across the human population (due to both vaccination efforts and natural infection) there could
393 eventually be selection for Spike mutations that result in substantial antigenic drift as seen for
394 Influenza. If and when this will happen is unpredictable given the current scale of ongoing
395 transmission worldwide. The data herein suggest evaluation of neutralizing mAbs from non-
396 overlapping binding clusters can highlight which Spike mutations will most impact sera
397 neutralization. Greater knowledge of the molecular epitopes recognized by individual mAbs
398 and their relative immunodominance within sera is needed urgently. This is because
399 understanding of rules of engagement for SARS-CoV-2 neutralizing antibodies is a crucial
400 component of preparedness for major antigenic changes and long-term management of
401 coronaviruses globally. Our findings stress the importance of continuous monitoring of variants
402 and in vitro assessment of their impact on neutralization. This is particularly relevant for the
403 use of convalescent plasma and the development of therapeutic monoclonal antibodies as well
404 as vaccine development and implementation.

405 **Acknowledgements**

406 The authors would like to thank James E Voss for the gift of HelaACE2 expressing cells, George
407 Kassiotis, Dan Frampton, Ann-Kathrin Reuschl and Joe Grove for helpful discussion and critical
408 feedback. We are indebted to the Biobank staff and study participants and their families at the
409 Royal Free Hospital, and the UCLH SAFER study recruitment team and study participants.

410

411 **Funding**

412 This study was funded by the UCL Coronavirus Response Fund made possible through
413 generous donations from UCL's supporters, alumni and friends (LEM) and also by the King's
414 Together Rapid COVID-19 Call award (KJD), the Huo Family Foundation (KJD). This research
415 was also funded by the Royal Free Charity. LEM is supported by a Medical Research Council
416 Career Development Award (MR/R008698/1). MJvG is a recipient of an AMC Fellowship, and
417 RWS is a recipient of a Vici grant from the Netherlands Organization for Scientific Research
418 (NWO). C.G. is supported by the MRC-KCL Doctoral Training Partnership in Biomedical Sciences

419 (MR/N013700/1). This work was also supported by National Institutes of Health grant P01
420 AI110657, and by the Bill and Melinda Gates Foundation grant INV-002022 (RWS). The work in
421 laboratory of PC was supported by the Francis Crick Institute (FC001061), which receives its
422 core funding from Cancer Research UK, the UK Medical Research Council, and the Wellcome
423 Trust. The SAFER study was funded by MRC UKRI (grant MC_PC_19082) and supported by the
424 UCLH/UCL NIHR BRC.

425 **Author contributions**

426 KJD, LEM, LM, SAG, PT, NL and CR-S characterized monoclonal antibodies and sera; AR, CR, and
427 PC expressed and purified proteins; JH, CH, HS and EN assembled the panels of human sera
428 samples; MJvG, RWS, YA, JLS isolated and provided monoclonal antibodies; RG generated and
429 provided mutated Spike plasmids, MJvG, KJD, and LEM wrote the paper with contributions from
430 all authors.

431 **Methods**

432 *Spike mutant generation*

433 QuikChange Lightening Site-Directed Mutagenesis kit was used to generate amino acid
434 substitutions in the SARS-CoV-2 Wuhan Spike expression vector (Seow et al., 2020) or the
435 D614G pCDNA Spike plasmid (S. A. Kemp et al., 2020) following the manufacturer's instructions
436 (Agilent Technologies, Inc., Santa Clara, CA). Spike B.1.1.7 was synthesised by Genewiz, Inc. and
437 cloned into the pCDNA expression vector using BamHI and EcoRI restriction sites.

438 *Neutralization assay*

439 HIV-1 particles pseudotyped with SARS-CoV-2 spike were produced in a T75 flask seeded the
440 day before with 3 million HEK293T cells in 10 ml complete DMEM, supplemented with 10%
441 FBS, 100 IU/ml penicillin and 100 µg/ml streptomycin. Cells were transfected using 60 µg of
442 PEI-Max (Polysciences) with a mix of three plasmids: 9.1 µg HIV-1 luciferase reporter vector
443 (Seow et al., 2020), 9.1 µg HIV p8.91 packaging construct and 1.4 µg WT SARS-CoV-2 spike
444 expression vector (Seow et al., 2020). Supernatants containing pseudotyped virions were
445 harvested 48 h post-transfection, filtered through a 0.45-µm filter and stored at -80°C.
446 Neutralization assays were conducted by serial dilution of monoclonal IgG at the indicated
447 concentrations in DMEM (10% FBS and 1% penicillin-streptomycin) and incubated with
448 pseudotyped virus for 1 h at 37°C in 96-well plates. HeLa cells stably expressing ACE-2
449 (provided by J.E. Voss, Scripps Institute) were then added to the assay (10,000 cells per 100 µl
450 per well). After 48-72 h luminescence was assessed as a proxy of infection by lysing cells with
451 the Bright-Glo luciferase kit (Promega), using a Glomax plate reader (Promega). Measurements
452 were performed in duplicate and used to calculate 50% inhibitory concentrations (IC₅₀) in
453 GraphPad Prism software.

454 *Semi-quantitative ELISA*

455 As described previously (O'Nions et al., 2020) nine columns of a half-well 96-well MaxiSorp
456 plate were coated with purified SARS-CoV-2 Spike S1 protein in PBS (3 µg/ml per well in 25 µL)
457 and the remaining three columns were coated with 25 µL goat anti-human F(ab)'2 diluted
458 1:1000 in PBS to generate the internal standard curve. After incubation at 4°C overnight, the
459 ELISA plate was blocked for 1 hour in assay buffer (PBS, 5% milk, 0.05% Tween 20). Sera was
460 diluted in assay buffer at dilutions from 1:50 to 1:5000 and 25 µL added to the ELISA plate.
461 Serial dilutions of known concentrations of IgG standards were applied to the three standard
462 curve columns in place of sera. The ELISA plate was then incubated for 2 hours at room
463 temperature and then washed 4 times with PBS-T (PBS, 0.05% Tween 20). Alkaline phosphatase-
464 conjugated goat anti-human IgG at a 1:1000 dilution was then added to each well and incubated
465 for 1 hour. Following this, plates were washed 6 times with PBS-T and 25 µL of colorimetric

466 alkaline phosphatase substrate added. Absorbance was measured at 405 nm. Antigen-specific
467 IgG concentrations in serum were then calculated based on interpolation from the IgG standard
468 results using a four-parameter logistic (4PL) regression curve fitting model.

469 *Serum samples*

470 SAFER study samples were collected as previously described (Houlihan et al., 2020). Data
471 derives from samples from 81 seropositive individuals during the first four months since
472 infection. The study protocol was approved by the NHS Health Research Authority (ref
473 20/SC/0147) on 26 March 2020. Ethical oversight was provided by the South- Central
474 Berkshire Research Ethics Committee. Serum samples from hospitalised patients were
475 obtained during their hospital stay and through the Tissue Access for Patient Benefit (TAPb)
476 scheme at The Royal Free Hospital (approved by UCL-Royal Free Hospital BioBank Ethical
477 Review Committee Reference number: NC2020.24 NRES EC number: 16/WA/0289).

478 **References**

479

480 Andreano, E., Piccini, G., Licastro, D., Casalino, L., Johnson, N. V., Paciello, I., . . . Rappuoli, R.
481 (2020). SARS-CoV-2 escape *in vitro* from a highly neutralizing COVID-19
482 convalescent plasma. *bioRxiv*.

483 Brouwer, P. J. M., Caniels, T. G., van der Straten, K., Snitselaar, J. L., Aldon, Y., Bangaru, S., . . . van
484 Gils, M. J. (2020). Potent neutralizing antibodies from COVID-19 patients define multiple
485 targets of vulnerability. *Science*, 369(6504), 643-650. doi:10.1126/science.abc5902

486 Burton, D. R., Poignard, P., Stanfield, R. L., & Wilson, I. A. (2012). Broadly Neutralizing
487 Antibodies Present New Prospects to Counter Highly Antigenically Diverse Viruses.
488 *Science*, 337, 183-186.

489 Cao, Y., Su, B., Guo, X., Sun, W., Deng, Y., Bao, L., . . . Xie, X. S. (2020). Potent Neutralizing
490 Antibodies against SARS-CoV-2 Identified by High-Throughput Single-Cell Sequencing
491 of Convalescent Patients' B Cells. *Cell*, 182(1), 73-84.e16. doi:10.1016/j.cell.2020.05.025

492 CDC. (2003). Update: Outbreak of severe acute respiratory syndrome--worldwide, 2003.
493 *MMWR Morb Mortal Wkly Rep*, 52(12), 241-246, 248.

494 Cevik, M., Kuppalli, K., Kindrachuk, J., & Peiris, M. (2020). Virology, transmission, and
495 pathogenesis of SARS-CoV-2. *BMJ*, 371.

496 Faria, N. R., Claro, I. M., Candido, D., Moyses Franco, L. A., Andrade, P. S., Coletti, T. M., . . . Sabino,
497 E. C., on behalf of CADDE Genomic Network. (2021). Genomic characterisation of an
498 emergent SARS-CoV-2 lineage in Manaus: preliminary findings.

499 Gralinski, L. E., & Menachery, V. D. (2020). Return of the Coronavirus: 2019-nCoV. *Viruses*,
500 12(2), 135.

501 Greaney, A. J., Loes, A. N., Crawford, K. H. D., Starr, T. N., Malone, K. D., Chu, H. Y., & Bloom, J. D.
502 (2021). Comprehensive mapping of mutations to the SARS-CoV-2 receptor-binding
503 domain that affect recognition by polyclonal human serum antibodies. *bioRxiv*.

504 Houlihan, C. F., Vora, N., Byrne, T., Lewer, D., Kelly, G., Heaney, J., . . . Nastouli, E. (2020).
505 Pandemic peak SARS-CoV-2 infection and seroconversion rates in London frontline
506 health-care workers. *Lancet*, 396(10246), e6-e7. doi:10.1016/s0140-6736(20)31484-7

507 Kemp, S., Datir, R., Collier, D., Ferreira, I., Carabelli, A., Harvey, W., . . . Gupta, R. (2020).
508 Recurrent emergence and transmission of a SARS-CoV-2 Spike deletion ΔH69/ΔV70.
509 *bioRxiv*.

510 Kemp, S. A., Collier, D. A., Datir, R., Ferreira, I. A., Gayed, S., Jahun, A., . . . Gupta, R. K. (2020).
511 Neutralising antibodies drive Spike mediated SARS-CoV-2 evasion. *medRxiv*.

512 Kidd, M., Richter, A., Best, A., Mirza, J., Percival, B., Mayhew, M., . . . McNally, A. (2020). S-variant
513 SARS-CoV-2 is associated with significantly higher viral loads in samples tested by
514 ThermoFisher TaqPath RT-QPCR. *medRxiv*.

515 Korber, B., Fischer, W. M., Gnanakaran, S., Yoon, H., Theiler, J., Abfalterer, W., . . . Montefiori, D. C.
516 (2020). Tracking Changes in SARS-CoV-2 Spike: Evidence that D614G Increases
517 Infectivity of the COVID-19 Virus. *Cell*. doi:10.1016/j.cell.2020.06.043

518 Lan, J., Ge, J., Yu, J., Shan, S., Zhou, H., Fan, S., . . . Wang, X. (2020). Structure of the SARS-CoV-2
519 spike receptor-binding domain bound to the ACE2 receptor. *Nature*, 581(7807), 215-
520 220. doi:10.1038/s41586-020-2180-5

521 Li, Q., Wu, J., Nie, J., Zhang, L., Hao, H., Liu, S., . . . Wang, Y. (2020). The Impact of Mutations in
522 SARS-CoV-2 Spike on Viral Infectivity and Antigenicity. *Cell*, 182(5), 1284-1294.e1289.
523 doi:10.1016/j.cell.2020.07.012

524 Li, W., Moore, M. J., Vasilieva, N., Sui, J., Wong, S. K., Berne, M. A., . . . Farzan, M. (2003).
525 Angiotensin-converting enzyme 2 is a functional receptor for the SARS coronavirus.
526 *Nature*, 426(6965), 450-454. doi:10.1038/nature02145

527 Lipsitch, M., Cohen, T., Cooper, B., Robins, J. M., Ma, S., James, L., . . . Murray, M. (2003).
528 Transmission Dynamics and Control of Severe Acute Respiratory Syndrome. *Science*,
529 300, 1966-1970.

530 Liu, H., Wu, N. C., Yuan, M., Bangaru, S., Torres, J. L., Caniels, T. G., . . . Wilson, I. A. (2020). Cross-
531 Neutralization of a SARS-CoV-2 Antibody to a Functionally Conserved Site Is Mediated
532 by Avidity. *Immunity*, 53(6), 1272-1280.e1275. doi:10.1016/j.jimmuni.2020.10.023

533 McMahan, K., Yu, J., Mercado, N. B., Loos, C., Tostanoski, L. H., Chandrashekhar, A., . . . Barouch, D.
534 H. (2020). Correlates of protection against SARS-CoV-2 in rhesus macaques. *Nature*.
535 doi:10.1038/s41586-020-03041-6

536 Mor, M., Werbner, M., Alter, J., Safra, M., Chomsky, E., Hada-Neeman, S., . . . Freund, N. T. (2020).
537 Multi-Clonal Live SARS-CoV-2 In Vitro Neutralization by Antibodies Isolated from
538 Severe COVID-19 Convalescent Donors. *bioRxiv*.

539 Ng, K. W., Faulkner, N., Cornish, G. H., Rosa, A., Harvey, R., Hussain, S., . . . Kassiotis, G. (2020).
540 Preexisting and de novo humoral immunity to SARS-CoV-2 in humans. *Science*,
541 370(6522), 1339-1343. doi:10.1126/science.abe1107

542 O'Nions, J., Muir, L., Zheng, J., Rees-Spear, C., Rosa, A., Roustan, C., . . . McCoy, L. E. (2020). SARS-
543 CoV-2 antibody responses in patients with acute leukaemia. *Leukemia*, 1-4.
544 doi:10.1038/s41375-020-01103-2

545 Ortega, J. T., Serrano, M. L., Pujol, F. H., & Rangel, H. R. (2020). Role of changes in SARS-CoV-2
546 spike protein in the interaction with the human ACE2 receptor: An in silico analysis.
547 *Excli j*, 19, 410-417. doi:10.17179/excli2020-1167

548 Oude Munnink, B. B., Sikkema, R. S., Nieuwenhuijse, D. F., Molenaar, R. J., Munger, E.,
549 Molenkamp, R., . . . Koopmans, M. P. G. (2020). Transmission of SARS-CoV-2 on mink
550 farms between humans and mink and back to humans. *Science*.

551 Petersen, E., Koopmans, M., Go, U., Hamer, D. H., Petrosillo, N., Castelli, F., . . . Simonsen, L.
552 (2020). Comparing SARS-CoV-2 with SARS-CoV and influenza pandemics. *The Lancet
553 Infectious Diseases*, 20(9), e238-e244. doi:10.1016/S1473-3099(20)30484-9

554 Plante, J. A., Liu, Y., Liu, J., Xia, H., Johnson, B. A., Lokugamage, K. G., . . . Shi, P.-Y. (2020). Spike
555 mutation D614G alters SARS-CoV-2 fitness. *Nature*. doi:10.1038/s41586-020-2895-3

556 Plotkin, S. A. (2008). Correlates of Vaccine-Induced Immunity. *Clinical Infectious Diseases*, 47(3),
557 401-409. doi:10.1086/589862

558 Polack, F. P., Thomas, S. J., Kitchin, N., Absalon, J., Gurtman, A., Lockhart, S., . . . Gruber, W. C.
559 (2020). Safety and Efficacy of the BNT162b2 mRNA Covid-19 Vaccine. *New England
560 Journal of Medicine*. doi:10.1056/NEJMoa2034577

561 Rambaut, A., Loman, N., Pybus, O., Barclay, W., Barrett, J., Carabelli, A., . . . Volz, E. (2020).
562 Preliminary genomic characterisation of an emergent SARS-CoV-2 lineage in the UK
563 defined by a novel set of spike mutations.

564 Robbiani, D. F., Gaebler, C., Muecksch, F., Lorenzi, J. C. C., Wang, Z., Cho, A., . . . Nussenzweig, M. C.
565 (2020). Convergent antibody responses to SARS-CoV-2 in convalescent individuals.
566 *Nature*, 584(7821), 437-442. doi:10.1038/s41586-020-2456-9

567 Rockx, B., Donaldson, E., Frieman, M., Sheahan, T., Corti, D., Lanzavecchia, A., & Baric, R. S.
568 (2010). Escape from human monoclonal antibody neutralization affects in vitro and in
569 vivo fitness of severe acute respiratory syndrome coronavirus. *J Infect Dis*, 201(6), 946-
570 955. doi:10.1086/651022

571 Rosa, A., Pye, V. E., Graham, C., Muir, L., Seow, J., Ng, K. W., . . . Cherepanov, P. (2021). SARS-CoV-
572 2 recruits a haem metabolite to evade antibody immunity. *In preparation*.

573 Seow, J., Graham, C., Merrick, B., Acors, S., Pickering, S., Steel, K. J. A., . . . Doores, K. J. (2020).
574 Longitudinal observation and decline of neutralizing antibody responses in the three
575 months following SARS-CoV-2 infection in humans. *Nat Microbiol*, 5(12), 1598-1607.
576 doi:10.1038/s41564-020-00813-8

577 Starr, T. N., Greaney, A. J., Hilton, S. K., Ellis, D., Crawford, K. H. D., Dingens, A. S., . . . Bloom, J. D.
578 (2020). Deep Mutational Scanning of SARS-CoV-2 Receptor Binding Domain Reveals
579 Constraints on Folding and ACE2 Binding. *Cell*, 182(5), 1295-1310.e1220.
580 doi:10.1016/j.cell.2020.08.012

581 Tegally, H., Wilkinson, E., Giovanetti, M., Iranzadeh, A., Fonseca, V., Giandhari, J., . . . de Oliveira,
582 T. (2020). Emergence and rapid spread of a new severe acute respiratory syndrome-

583 related coronavirus 2 (SARS-CoV-2) lineage with multiple spike mutations in South
584 Africa. *medRxiv*.

585 Weisblum, Y., Schmidt, F., Zhang, F., DaSilva, J., Poston, D., Lorenzi, J. C., . . . Bieniasz, P. D. (2020).
586 Escape from neutralizing antibodies by SARS-CoV-2 spike protein variants. *Elife*, 9.
587 doi:10.7554/eLife.61312

588 Weissman, D., Alameh, M.-G., de Silva, T., Collini, P., Hornsby, H., Brown, R., . . . Montefiori, D. C.
589 (2020). D614G Spike Mutation Increases SARS CoV-2 Susceptibility to Neutralization.
590 *Cell Host & Microbe*. doi:<https://doi.org/10.1016/j.chom.2020.11.012>

591 Welkers, M. R. A., Han, A. X., Reusken, C. B. E. M., & Eggink, D. (2020). Possible host-adaptation
592 of SARS-CoV-2 due to improved ACE2 receptor binding in mink. *Virus evolution*.
593 doi:10.1093/ve/veaa094

594 Wu, N. C., Yuan, M., Bangaru, S., Huang, D., Zhu, X., Lee, C. D., . . . Wilson, I. A. (2020). A natural
595 mutation between SARS-CoV-2 and SARS-CoV determines neutralization by a cross-
596 reactive antibody. *PLoS Pathog*, 16(12), e1009089. doi:10.1371/journal.ppat.1009089

597 Xie, X., Zou, J., Fontes-Garfias, C. R., Xia, H., Swanson, K. A., Cutler, M., . . . Shi, P.-Y. (2021).
598 Neutralization of N501Y mutant SARS-CoV-2 by BNT162b2 vaccine-elicited sera.
599 *bioRxiv*.

600 Xu, C., Wang, Y., Liu, C., Zhang, C., Han, W., Hong, X., . . . Cong, Y. (2021). Conformational
601 dynamics of SARS-CoV-2 trimeric spike glycoprotein in complex with receptor ACE2
602 revealed by cryo-EM. *Science Advances*, 7.

603 Yi, C., Sun, X., Ye, J., Ding, L., Liu, M., Yang, Z., . . . Sun, B. (2020). Key residues of the receptor
604 binding motif in the spike protein of SARS-CoV-2 that interact with ACE2 and
605 neutralizing antibodies. *Cellular & Molecular Immunology*, 17(6), 621-630.
606 doi:10.1038/s41423-020-0458-z

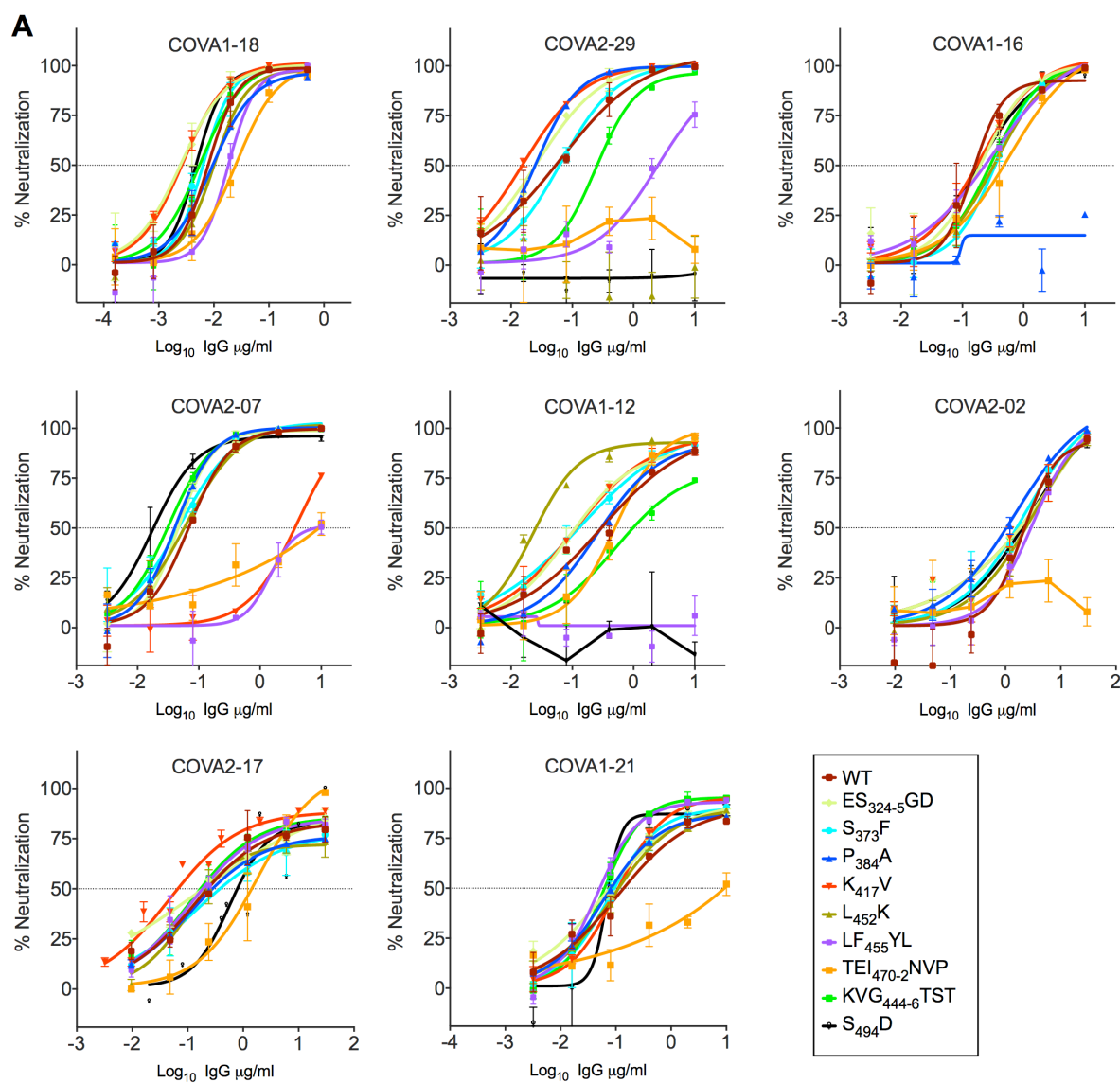
607 Zost, S. J., Wu, N. C., Hensley, S. E., & Wilson, I. A. (2019). Immunodominance and Antigenic
608 Variation of Influenza Virus Hemagglutinin: Implications for Design of Universal
609 Vaccine Immunogens. *The Journal of Infectious Diseases*, 219(Supplement_1), S38-S45.
610 doi:10.1093/infdis/jiy696.

611

612 **Figures**

613 **Figure 1: Mutating amino acids in SARS-CoV-2 Spike to match SARS-CoV decreases mAb**
614 **neutralization. (A)** Indicated mAbs were serially diluted in duplicate and incubated with each
615 mutant SARS-CoV-2 luciferase-encoding pseudotyped virus (as noted in the legend) prior to the
616 addition of HeLa cells expressing ACE-2. After two days, neutralization was measured as the
617 relative reduction in relative light units (RLU). Data are representative of three independent
618 repeats. The horizontal dotted line on each graph indicates 50% neutralization. **(B)** 50%
619 inhibitory concentration (IC_{50}) values were calculated for each mAb against the mutant SARS-
620 CoV-2 pseudotyped viruses indicated in the left hand column. IC_{50} values are color-coded as
621 follows: pale grey $>1\mu\text{g}/\text{ml}$, light grey $0.1\text{-}1\mu\text{g}/\text{ml}$, medium grey $0.1\text{-}0.01\mu\text{g}/\text{ml}$ and dark grey
622 $<0.01\mu\text{g}/\text{ml}$. The previously established binding cluster for each mAb is indicated above each
623 column, and whether or not the mAb binds RBD is also indicated.

624 **FIGURE 1**



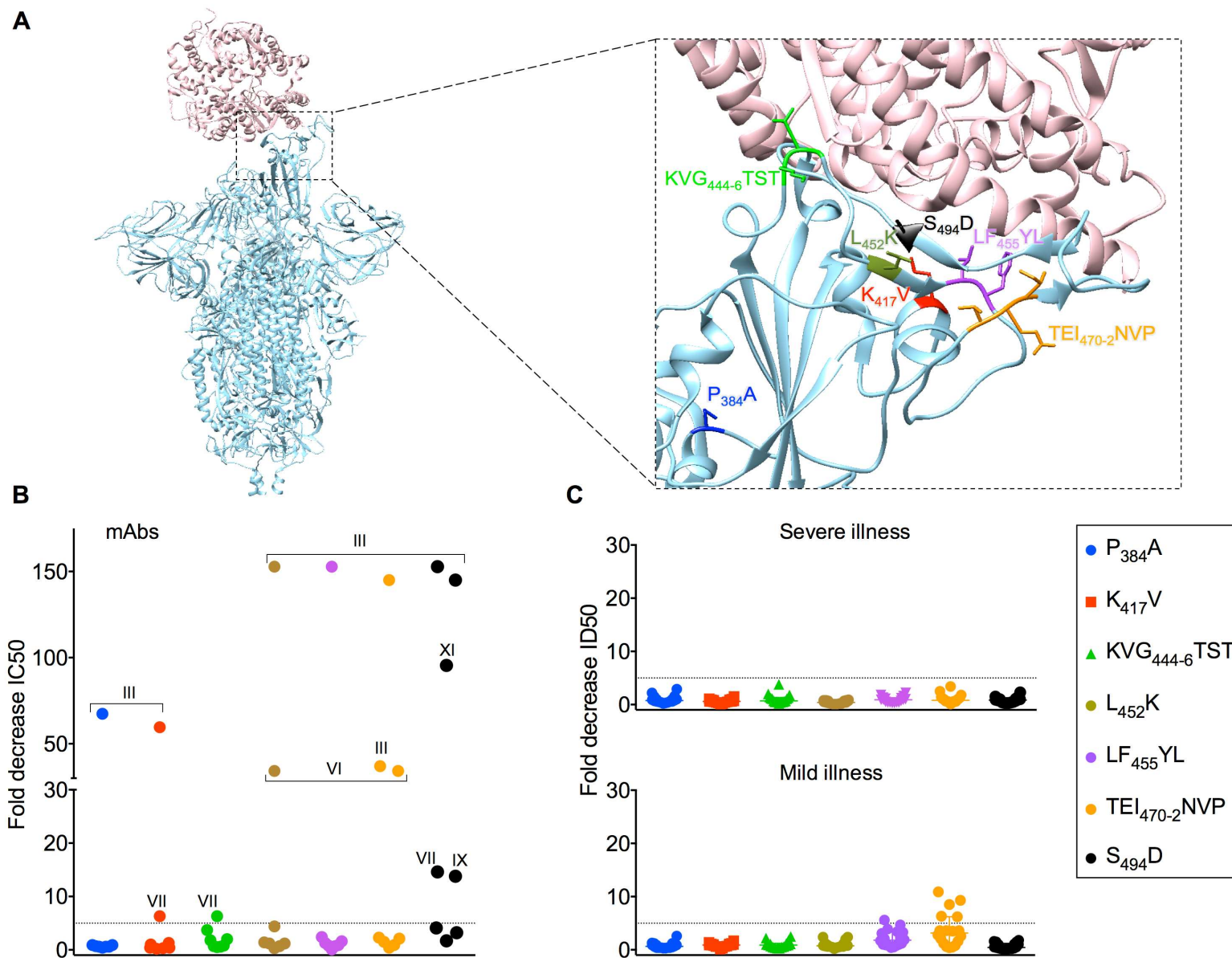
B

RBD

| | RBD | | | | | | | | | | | |
|--------------------------|-----------|----------|-------------|----------|------------|----------|-------------|----------|------------|--|------------|--|
| | Cluster I | | Cluster III | | Cluster VI | | Cluster VII | | Cluster IX | | Cluster XI | |
| | COVA1-18 | COVA2-29 | COVA1-16 | COVA2-07 | COVA1-12 | COVA2-02 | COVA2-17 | COVA1-21 | | | | |
| ES ₃₂₄₋₅ GD | 0.003 | 0.027 | 0.203 | 0.046 | 0.087 | 12.930 | 0.161 | 0.062 | | | | |
| S ₃₇₃ F | 0.006 | 0.064 | 0.351 | 0.050 | 0.139 | 2.230 | 0.144 | 0.076 | | | | |
| P ₃₈₄ A | 0.005 | 0.025 | >10 | 0.041 | 0.255 | 1.514 | 0.115 | 0.060 | | | | |
| K ₄₁₇ V | 0.003 | 0.016 | 0.190 | 4.113 | 0.106 | 12.930 | 0.047 | 0.103 | | | | |
| KVG ₄₄₄₋₆ TST | 0.006 | 0.244 | 0.299 | 0.032 | 0.529 | 12.930 | 0.111 | 0.059 | | | | |
| L ₄₅₂ K | 0.010 | >10 | 0.355 | 0.061 | 0.023 | 3.238 | 0.096 | 0.087 | | | | |
| LF ₄₅₅ YL | 0.018 | 2.423 | 0.311 | >10 | >10 | 3.130 | 0.117 | 0.046 | | | | |
| TEI ₄₇₀₋₂ NVP | 0.025 | >10 | 0.603 | >10 | 0.506 | >30 | 1.810 | 10.000 | | | | |
| S ₄₉₄ D | 0.009 | >10 | 0.185 | 0.017 | >10 | 2.777 | 0.577 | 0.068 | | | | |
| Wildtype | 0.008 | 0.065 | 0.148 | 0.069 | 0.292 | 2.048 | 0.131 | 0.105 | | | | |

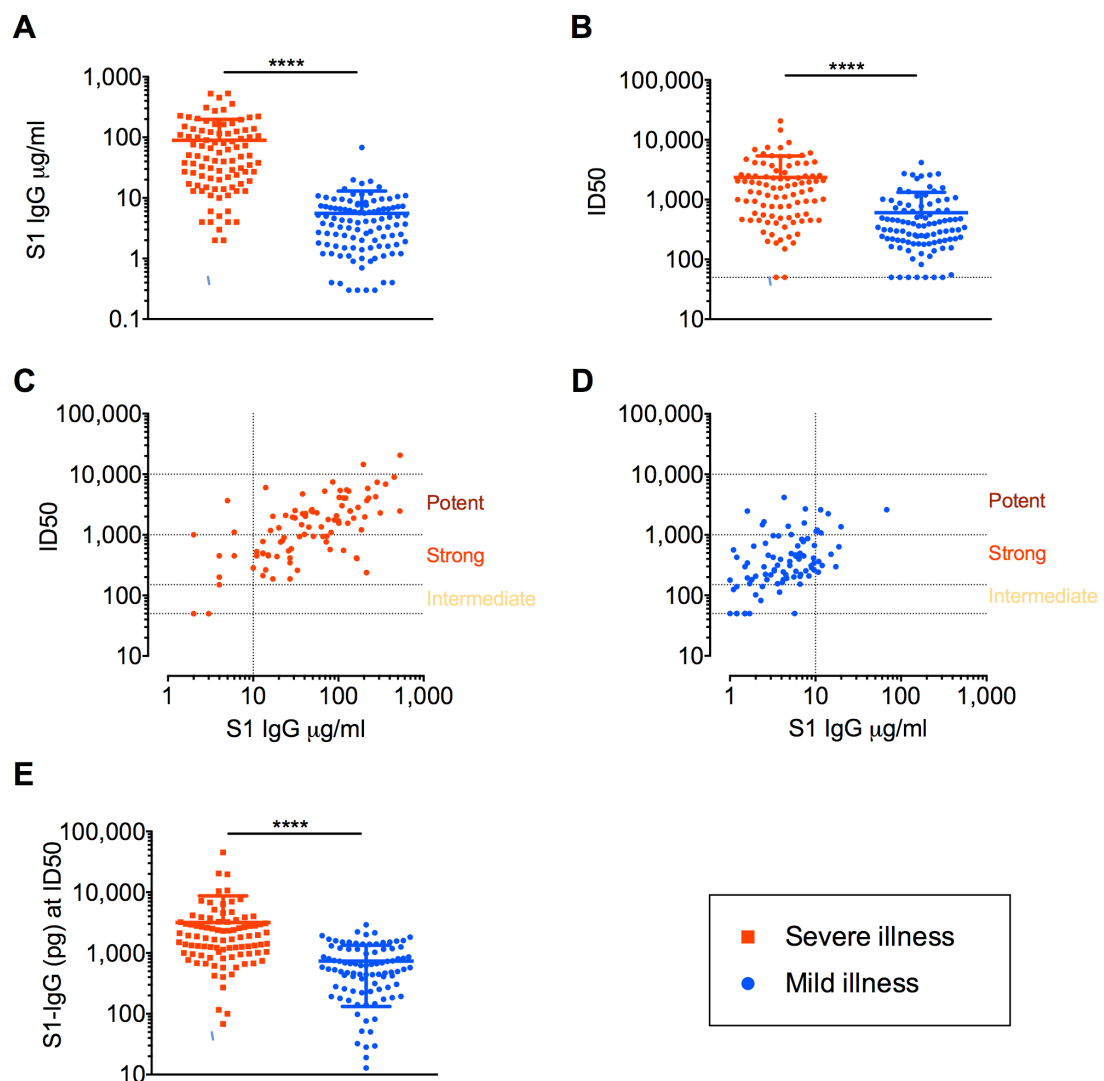
624 **Figure 2: Neutralization by sera is less adversely affected by SARS-CoV amino acid**
625 **substitutions in SARS-CoV-2 Spike. (A)** Representation of SARS CoV-2 Spike trimer (blue) in
626 complex with ACE-2 (pink) (PDB code 7DF4). Magnified image shows mutated amino acid side
627 chains at residues of interest. **(B)** IC_{50} values for each mAb against SARS-CoV-2 wildtype
628 pseudotyped virus were divided by the IC_{50} for each mutant pseudotyped virus against the
629 corresponding mAb to generate the fold decrease in neutralization on the Y-axis. The dotted
630 horizontal line indicates a 5-fold drop in neutralization potency. The competitive binding
631 clusters of each mAb that loses > 5-fold neutralization activity are labeled on the graph. **(C)**
632 Thirty six serum samples were serially titrated and incubated with the mutant SARS-CoV-2
633 luciferase-encoding pseudotyped viruses indicated in the legend prior to the addition of HeLa
634 cells expressing ACE-2. After two days, neutralization was measured as the relative reduction in
635 relative light units (RLU) and 50% inhibitory dilution factors calculated using Graphpad Prism.
636 ID_{50} values for each sera against SARS-CoV-2 wildtype pseudotyped virus were divided by the
637 ID_{50} for each mutant pseudotyped virus against the corresponding sera to generate the fold
638 decrease in neutralization on the Y-axis. The dotted horizontal line indicates a 5-fold drop in
639 neutralization potency. The 18 serum samples from hospitalized patients are shown in the
640 upper graph labeled “severe illness” and the 18 serum samples from healthcare workers who
641 experience mild/asymptomatic COVID-19 are shown in the lower graph labeled “mild illness”.

643 FIGURE 2



643 **Figure 3: Serum responses following severe COVID-19 have greater polyclonality but less**
644 **efficient neutralization. (A)** Spike S1 subunit semi-quantitative titers measured by ELISA (see
645 Methods) are shown on the Y-axis for 94 serum samples from hospitalized COVID-19 patients
646 and 105 serum samples from healthcare workers who experienced mild COVID-19 disease. **(B)**
647 Serum ID₅₀ values measured by pseudotyped neutralization assay (see Methods) are shown on
648 the X-axis for 93 serum samples from hospitalized COVID-19 patients and 99 serum samples
649 from healthcare workers who experienced mild COVID-19 disease. Note, some serum samples
650 from the original cohort that had binding titers gave no neutralization titer (6 from healthcare
651 workers, 1 from a hospitalized patient). **(C)** ID₅₀ values measured by pseudotyped
652 neutralization assay for serum samples from hospitalized COVID-19 patients plotted on the Y-
653 axis against the corresponding S1 IgG binding titer for each sample. Relative ranking of
654 neutralization titers is indicated on the graph. **(D)** Serum ID₅₀ values measured by pseudotyped
655 neutralization assay for the serum samples from healthcare workers who experienced mild
656 COVID-19 disease are plotted on the Y-axis against the corresponding S1 IgG binding titer for
657 each sample. Relative ranking of neutralization titers is indicated on the graph. Only sera that
658 gave a measurable titer in both semi-quantitative ELISA or pseudotype neutralization assay
659 were included in (B), (C) and (D). Serum sample groups are color-coded according to the
660 legend. **(E)** Concentrations of S1-specific serum IgG (pg) at ID₅₀ dilutions were calculated using
661 the IgG titers quantified via the semi-quantitative ELISA and the known ID₅₀ value. Only sera
662 that gave a measurable titer in both semi-quantitative ELISA and pseudotype neutralization
663 assay were included. Data for (A)–(B) and (E) were analyzed by a non-parametric Mann-
664 Whitney U test.

666 **FIGURE 3**



666 **Figure 4: Variant B.1.1.7 SARS-CoV-2 Spike effect on mAb and serum neutralization. (A)**
667 Indicated mAbs were serially diluted in duplicate and incubated with the mutant SARS-CoV-2
668 luciferase-encoding pseudotyped virus in the legend prior to the addition of HeLa cells
669 expressing ACE-2. After two days neutralization was measured as the relative reduction in
670 relative light units (RLU). Data are representative of three independent repeats. The horizontal
671 dotted line on each graph indicates 50% neutralization. **(B)** IC₅₀ values for each mAb or ID₅₀
672 values for each serum sample against SARS-CoV-2 D₆₁₄G pseudotyped virus were divided by the
673 IC₅₀ for each mutant pseudotyped virus against the corresponding mAb to generate the fold
674 decrease in neutralization on the Y-axis, as color-coded in the key. The dotted horizontal line
675 indicates a 5-fold drop in neutralization potency. Whether fold decrease in neutralization
676 potency refers to mAbs, 18 serum samples from hospitalized patients or 18 serum samples
677 from healthcare workers who experience mild/asymptomatic COVID-19 is indicated under the
678 graph by the labels “mAbs”, “severe illness” and “mild illness”, respectively.

680 **FIGURE 4**

